PANCREAS

Quantitative MRI of chronic pancreatitis: results from a multi-institutional prospective study, magnetic resonance imaging as a non-invasive method for assessment of pancreatic fibrosis (MINIMAP)

Temel Tirkes[1] · Dhiraj Yadav[2] · Darwin L. Conwell[3] · Paul R. Territo[4] · Xuandong Zhao[5] · Scott A. Persohn[6] · Anil K. Dasyam[7] · Zarine K. Shah[8] · Sudhakar K. Venkatesh[9] · Naoki Takahashi[9] · Ashley Wachsman[10] · Liang Li[11] · Yan Li[12] · Stephen J. Pandol[13] · Walter G. Park[14] · Santhi S. Vege[15] · Phil A. Hart[16] · Mark Topazian[17] · Dana K. Andersen[18] · Evan L. Fogel[19] · On behalf of the Consortium for the Study of Chronic Pancreatitis, Diabetes, Pancreatic Cancer (CPDPC)

Abstract

Purpose To determine if quantitative MRI techniques can be helpful to evaluate chronic pancreatitis (CP) in a setting of multi-institutional study.

Methods This study included a subgroup of participants ($n = 101$) enrolled in the Prospective Evaluation of Chronic Pancreatitis for Epidemiologic and Translational Studies (PROCEED) study (NCT03099850) from February 2019 to May 2021. MRI was performed on 1.5 T using Siemens and GE scanners at seven clinical centers across the USA. Quantitative MRI parameters of the pancreas included T1 relaxation time, extracellular volume (ECV) fraction, apparent diffusion coefficient (ADC), and fat signal fraction. We report the diagnostic performance and mean values within the control ($n = 50$) and CP ($n = 51$) groups. The T1, ECV and fat signal fraction were combined to generate the quantitative MRI score (Q-MRI).

Results There was significantly higher T1 relaxation time; mean 669 ms (± 171) vs. 593 ms (± 82) ($p = 0.006$), ECV fraction; 40.2% (± 14.7) vs. 30.3% (± 11.9) ($p < 0.001$), and pancreatic fat signal fraction; 12.2% (± 5.5) vs. 8.2% (± 4.4) ($p < 0.001$) in the CP group compared to controls. The ADC was similar between groups ($p = 0.45$). The AUCs for the T1, ECV, and pancreatic fat signal fraction were 0.62, 0.72, and 0.73, respectively. The composite Q-MRI score improved the diagnostic performance (cross-validated AUC: 0.76).

Conclusion Quantitative MR parameters evaluating the pancreatic parenchyma (T1, ECV fraction, and fat signal fraction) are helpful in the diagnosis of CP. A Q-MRI score that combines these three MR parameters improves diagnostic performance. Further studies are warranted with larger study populations including patients with acute and recurrent acute pancreatitis and longitudinal follow-ups.

Extended author information available on the last page of the article

Graphical abstract
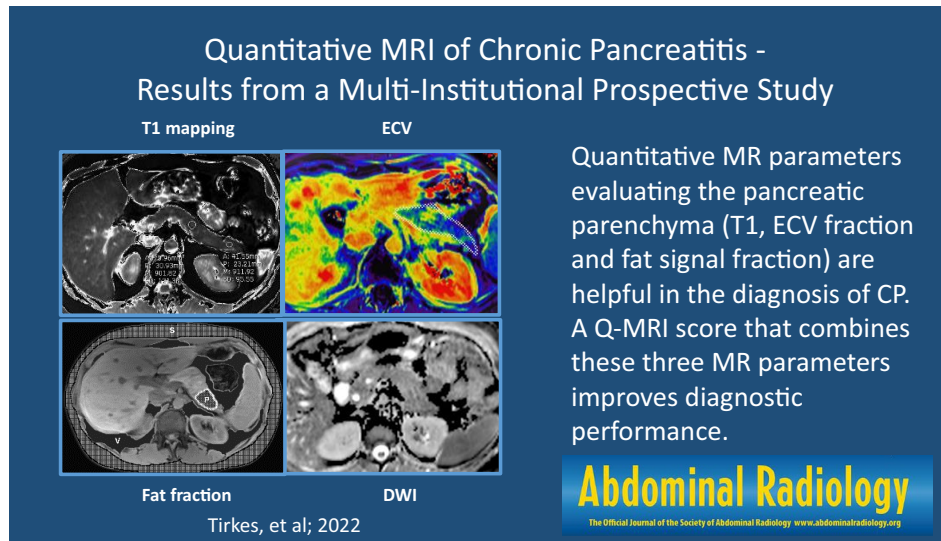
Abbreviations

CP	Chronic pancreatitis
MRI	Magnetic resonance imaging
Q-MRI	Quantitative MRI
ECV	Extracellular volume
DWI	Diffusion-weighted imaging
ADC	Apparent diffusion coefficient
MRCP	Magnetic resonance cholangiopancreatography
CPDPC	Consortium for the study of chronic pancreatitis, diabetes, and pancreatic cancer
MINIMAP	Magnetic resonance imaging as a non-invasive method for the assessment of pancreatic fibrosis

Introduction

The histologic hallmarks of CP include fibrosis, loss of acinar and islet cells and ductal changes [1]. Since histology is not easily or readily available in clinical practice, cross-sectional imaging studies, such as computerized tomography (CT) and Magnetic Resonance Imaging (MRI) with or without Magnetic Resonance Cholangiopancreatography (MRCP) are recommended by the American College of Gastroenterology as the first line diagnostic modalities [2]. Using MRCP for Cambridge classification results in variable interpretation [3] with a moderate interobserver agreement [4, 5]. Pancreatic ducts are a small fraction of the entire pancreas, and ductal imaging alone does not reflect the parenchymal fibrosis or acinar cell loss described in histopathology. Hence, diagnosis of CP can be elusive and delayed in patients without moderate-to-severe ductal abnormalities on MRCP or calcifications seen on CT. Prior retrospective studies, expert panel reviews, and consensus guidelines have suggested that parenchymal MRI findings such as T1 signal intensity ratio and quantitative relaxation time, pancreas volume, fat fraction, extracellular volume fraction can be helpful for diagnostic evaluation of CP [6–10]. In addition, quantitative MR imaging offers several advantages over conventional non-quantitative imaging, including quantitative measurement of the tissue relaxometry values (in vivo characterization of tissues), simplicity of analysis by allowing population-based comparisons, and cross-platform compatibility [11].

We present the results of a multi-institutional pilot study, Magnetic Resonance Imaging as a Non-Invasive Method for the Assessment of Pancreatic Fibrosis (MINIMAP) [12], funded by the National Institute of Diabetes and Digestive and Kidney Diseases (NIDDK) as an ancillary study within the Consortium for the Study of Chronic Pancreatitis, Diabetes, and Pancreatic Cancer (CPDPC) [13, 14]. Our aim

with the MINIMAP study was to explore the potential of quantitative parenchymal MRI features serving as a non-invasive imaging biomarker for CP [12].

Materials and methods

Study population

We enrolled a subset of adults from seven clinical centers participating in the CPDPC longitudinal cohort study Prospective Evaluation of Chronic Pancreatitis for Epidemiologic and Translational Studies (PROCEED) (NCT03099850). An IRB approval was obtained at each center and all participants signed a written informed consent form prior to the study procedures [15]. The study was performed at seven participating centers: Indiana University in Indianapolis, IN, University of Pittsburgh Medical Center in Pittsburgh, PA, The Ohio State University Wexner Medical Center in Columbus, OH, Mayo Clinic in Rochester, MN, Stanford University in Stanford, CA, Cedars-Sinai Medical Center in Los Angeles, CA, University of California Los Angeles Medical Center in Los Angeles, CA. The Data Coordinating Center which provided the statistical support was in The University of Texas MD Anderson Cancer Center in Houston, TX. All the participants provided informed consent before any study procedures were performed. The MINIMAP study protocol has been published and includes the patient enrollment algorithm with a flow diagram, inclusion/exclusion criteria, sample size calculation, and data collection points [12]. A total of 137 control and CP group participants agreed and signed consent from February 2019 to May 2021, and 123 completed the imaging. After excluding 22 MRIs for reasons listed in Fig. 1, 101 MRIs were available for image analysis. These MR examinations were from 50 healthy controls (no abdominal symptoms and no personal or family history of pancreatic disease) and 51 participants with definite CP (Cambridge stage 3 or 4 by MRCP or presence of calcifications on CT scan).

MR imaging

All MRI examinations were performed on 1.5T using Siemens or GE scanners. MRI protocol is available in Table S1 of the Supplemental Materials section. The study imaging protocol and image reconstruction steps were published separately [12].
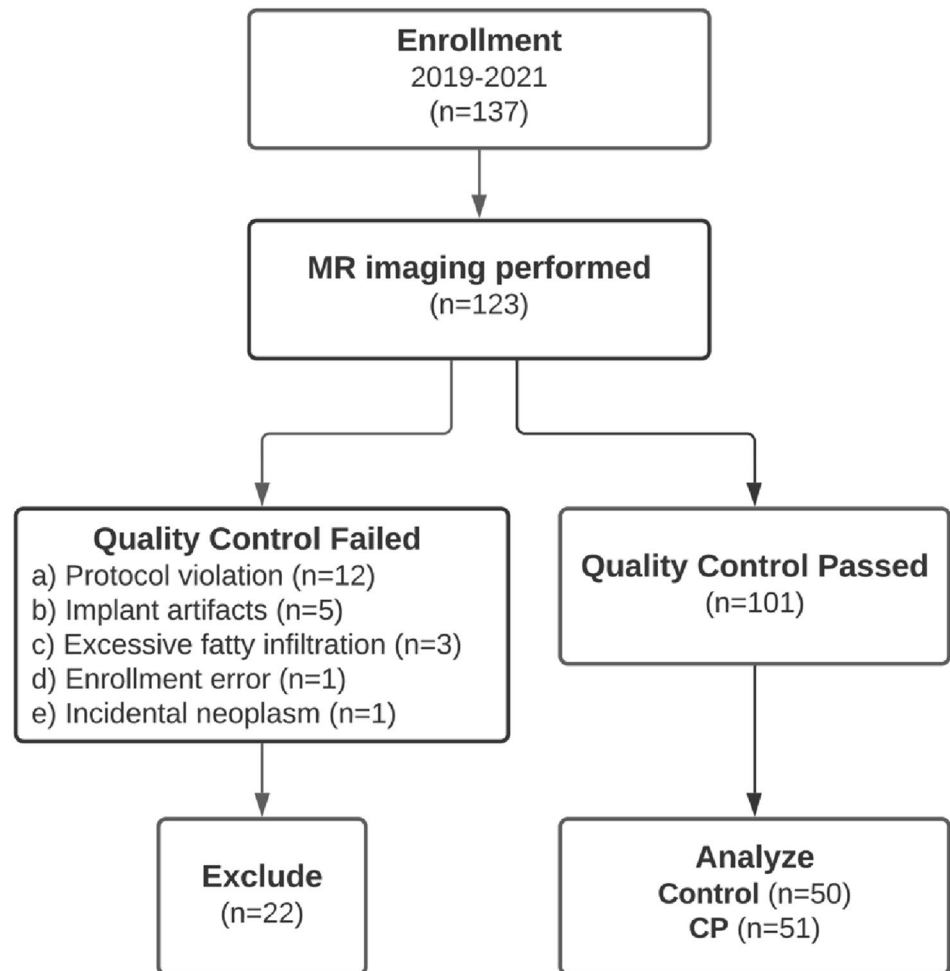
Image analysis

An image analysis scientist with 17 years of experience who was blinded to the clinical information and cohort assignment performed pancreatic volume measurement. Images were imported into MIM (v7.05, MIM Software, Beachwood OH), and multi-flip angle images with and without contrast enhancement were co-registered via manual registration and exported as DICOM files. Post-registration, the abdominal aorta was manually segmented from arterial phase contrast-enhanced T1-weighted VIBE-DIXON images and image mask at the level of the pancreas were exported as DICOM images. To compute B1 field corrected spin–lattice relaxation (T1) parametric maps, registered multi-flip angle single-shot echo-planar B1 images (i.e., 60° and 120°), T1-weighted VIBE-DIXON without (i.e., 3° and 19° degrees) and with (i.e., 5° and 29°) contrast, along with aorta masks were imported into custom in-house developed and validated software. For details of B1 corrections to improve image homogeneity not provided by the instrumentation, voxel-wise corrections on multi-flip angle images were computed as described in the supplemental materials. To compute T1 maps plus and minus contrast enhancement, voxel-wise parametric maps were computed according to established protocols, where the details are presented in the supplemental materials. Finally, using the T1 maps plus and minus contrast enhancement, along with an aortic mask at the level of the pancreas, ECV parametric maps were computed per voxel, where the detailed formulation is described in the Supplemental Materials section. Examples of T1 and ECV maps are shown in Fig. 2.

Statistical analysis

Two-sample t-test was used to test mean differences in MRI parameters between controls and participants with CP. Receiver Operating Characteristics (ROC) curve analysis was used to assess the diagnostic performance. We fit a logistic regression with the disease status (CP vs. control) as the dependent variable, and T1 mapping, ECV, and pancreatic fat signal fraction as the independent variables. Sporadic missing values in the ECV and pancreatic fat signal fraction were imputed by the available data in the control or CP groups. The linear predictor of this model forms the optimal combination of these three MRI parameters [16], called the Quantitative MRI (Q-MRI) score. To protect against overfitting, we used 200 bootstrap cross-validation

Fig. 1 Flowchart of participant enrollment in the Magnetic Resonance Imaging as a Non-invasive Method for the Assessment of Pancreatic Fibrosis (MINIMAP) study. Fourteen participants declined imaging after enrollment due to the COVID-19 pandemic

Enrollment
2019-2021
(n=137)

MR imaging performed
(n=123)

Quality Control Failed
a) Protocol violation (n=12)
b) Implant artifacts (n=5)
c) Excessive fatty infiltration (n=3)
d) Enrollment error (n=1)
e) Incidental neoplasm (n=1)

Quality Control Passed
(n=101)

Exclude
(n=22)

Analyze
Control (n=50)
CP (n=51)

to calculate the area under the curve (AUC) of the Q-MRI. The control and CP groups differed in their population characteristics. To remove their confounding effects, we used propensity score weighting to balance the distribution of selected demographics and behavioral covariates between CP and control, and a weighted ROC analysis was conducted [17]. Specifically, we estimated the propensity score by the covariate balancing propensity score (CBPS) algorithm [18] with inverse probability weights. The covariates in the propensity score model include age, BMI, gender, race (white, black, other, unreported), smoking status (never, past, current), history of drinking alcohol (never, past, current), drinking category (abstainer, light, moderate, heavy, very heavy, unknown) and quadratic terms of age and body mass index (BMI). We assessed covariate balance before and after propensity score weighting by the standardized differences (S/D), i.e., the mean difference divided by the pooled standard deviation, expressed as a percentage. Due to the small sample size, we did not calculate the cross-validated AUC of Q-MRI from propensity score analysis. We performed linear regression to study the association between each MRI parameter and demographics, behavior and clinical covariates among the CP participants. The covariates included the variables used in propensity score adjustment as well as additional clinical variables related to CP, including pancreatic calcification, diabetes, and exocrine pancreatic dysfunction (EPD).

Results

Table 1 summarizes the demographic, behavioral, and clinical characteristics of controls and participants with CP. Compared with controls, participants with CP were older
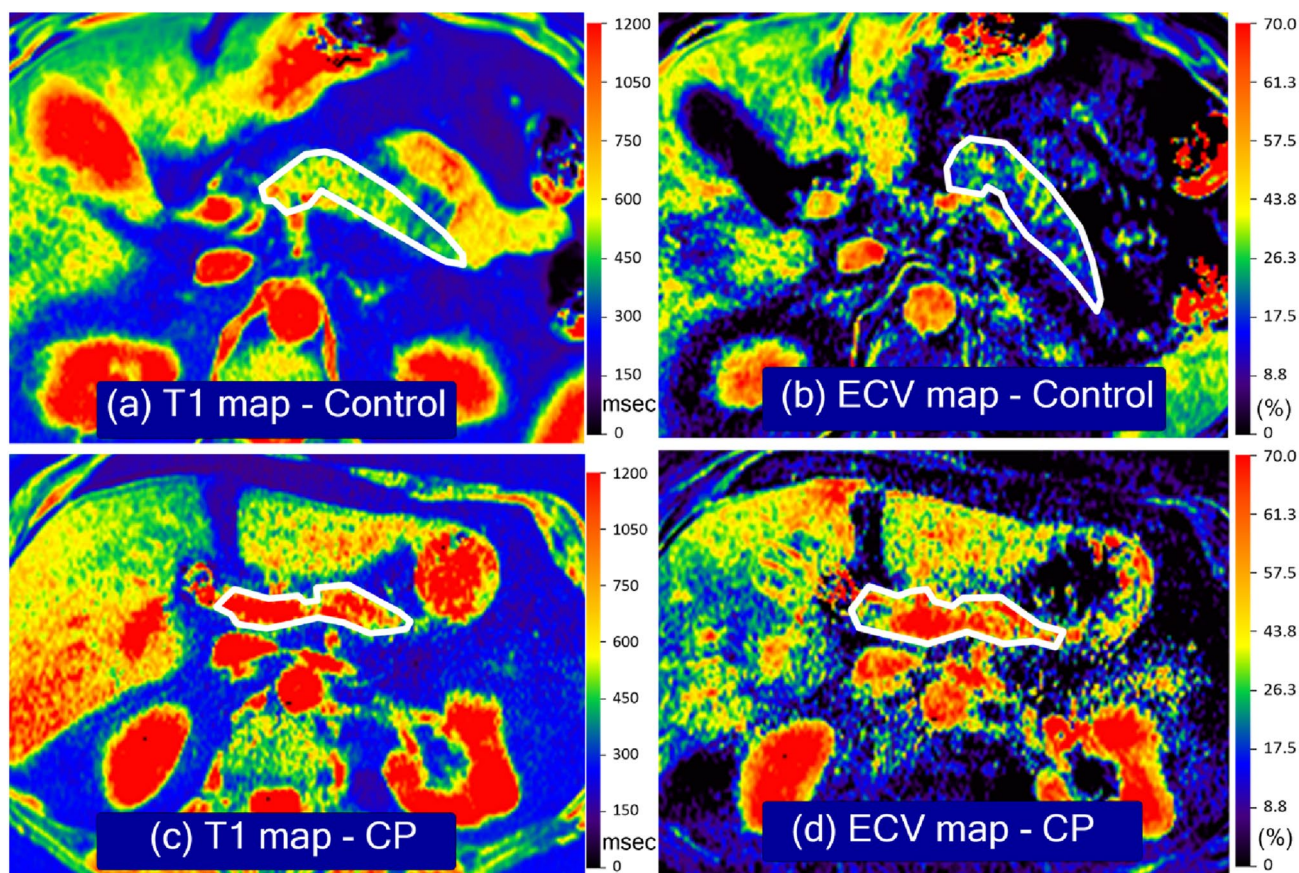
Fig. 2 T1 and extracellular volume (ECV) maps in the control and chronic pancreatitis (CP) groups. **a** is a T1 map and **b** is the ECV map of a healthy control group participant who is a 49-year-old female with no symptoms. **c** is the T1 map, and **d** is the ECV map of a 42-year-old female with a history of CP. Units for the T1 maps are msec, and the ECV maps use fractions. Relatively higher T1 relaxation times and ECV fractions seen in participants with CP are depicted as orange and red pixels

$(53.9 \pm 14.6$ vs. 50.3 ± 14.0 years) and more likely to be female (49.8% vs 42%), white (91.8% vs. 82.6%), current smoker (18.0% vs. 12.8%), never drinker (24.0% vs. 10.6%), or past drinker (48.0% vs. 12.8%). Among participants with CP, diabetes, pancreatic calcifications, and EPD were present in 28.0%, 52.0%, and 23.3%, respectively. None of the participants in the control group had diabetes.

T1 mapping, ECV, pancreatic fat signal fraction, and apparent diffusion coefficient (ADC)

Figure 3 and Table 2 show the differences of T1 relaxation time, ECV, pancreatic fat signal fraction and Q-MRI between control and CP. In the CP group, there was a significant increase in the mean $(\pm SD)$ T1 relaxation time of 669 (± 171) vs. 593 (± 82) msec, $(p = 0.006)$, ECV of 40.2% (± 14.7) vs. 30.3% (± 11.9) $(p < 0.001)$, and pancreatic fat signal fraction of 12.2% (± 5.5) vs. 8.2% (± 4.4) $(p < 0.001)$. However, mean ADC was very similar between groups; 1771 (± 404) vs 1,703 (± 443) 10^{-6} mm^2/s, $(p = 0.46)$. The ROC curves (Fig. 4a) showed moderately large AUC in T1 mapping (0.618), ECV (0.715), and pancreatic fat signal fraction (0.727), but low AUC in ADC (0.538).

Q-MRI score

Figure 3e and Table 2 compare the performance of the Q-MRI score between the control and CP groups. The Q-MRI was higher among the CP, with a mean value of 0.80 for CP and − 0.56 for the control group $(p < 0.001)$.

Table 1 Baseline characteristics of controls and participants with CP

Patient characteristics	Controls ($n=50$)	CP ($n=51$)	p-value*
Age (in years), mean (SD)	50.3 (14.0)	53.9 (14.6)	0.20
BMI (kg/m^2), mean (SD)	27.0(4.9)	26.9 (5.5)	0.79
Male, n (%)	26 (52.0)	21 (41.2)	0.32
Race, n (%)			
White	38 (82.6)[4]	45 (91.8)[2]	0.38
Black	5 (10.9)	2 (4.1)	
Asian	3 (6.5)	2 (4.1)	
Smoking, n (%)			
Never	29 (61.7)[3]	27 (54.0)[1]	0.72
Past	12 (25.5)	14 (28.0)	
Current	6 (12.8)	9 (18.0)	
Drinking, n (%)			
Never	5 (10.6)[3]	12 (24.0)[1]	< 0.001
Past	6 (12.8)	24 (48.0)	
Current	36 (76.6)	14 (28.0)	
Drinking category, n (%)			
Abstainer	5 (12.2)[9]	12 (25.0)[3]	0.57
Light	6 (14.6)	8 (16.7)	
Moderate	12 (29.3)	10 (20.8)	
Heavy	13 (31.7)	14 (29.2)	
Very heavy	5 (12.2)	4 (8.3)	
Alcohol etiology, n (%)			
No		42 (84.0)[1]	N/A
Yes		8 (16.0)	
Diabetes mellitus, n (%)			
No		36 (72.0)[1]	N/A
Yes		14 (28.0)	
Calcifications, n (%)			
No		24 (48.0)[1]	N/A
Yes		26 (52.0)	
Exocrine pancreatic dysfunction (EPD), n (%)			
No		23 (76.7)	N/A
Yes		7 (23.3)	
Not tested**		21	

Mean (standard deviation) are reported for age and BMI. Count (column percentage) are reported for categorical variables

Superscripts indicate the counts of undocumented/unreported values, which are excluded from the percentage calculation

*Wilcoxon test for continuous variables and Fisher exact test for categorical variables

**CP participants with no known EPD who did not undergo a per-protocol assessment after enrollment for EPD with fecal elastase testing

The estimated AUC from internal cross-validation was 0.76 (Table 2), slightly smaller than without cross-validation (0.78; Fig. 4a) but notably higher than any of the individual MRI parameters that make up the Q-MRI.

Propensity score adjusted ROC analysis of the four MRI parameters

The CP and control groups differed in their demographic and behavioral characteristics (Table 1, Table S2). Conventionally, an S/D less than 5% is considered an acceptable balance. In Table S2, 15 of 17 covariates had S/D of more than 5%, with a large imbalance noted in some covariates (e.g., 88.7% in current drinking). The covariate imbalance confounds the association between the MRI parameters and the CP, which motivates the use of propensity score weighting to reduce the imbalance. The resulting weighted AUC quantifies the expected difference in MRI parameters between control and CP groups when the two populations have similar demographic and behavioral characteristics. The weighted AUCs were 0.652, 0.676, 0.742, 0.497, and 0.748 for T1, ECV, pancreatic fat signal fraction, ADC, and Q-MRI, respectively (Fig. 4b). The proposed propensity score procedure effectively reduced S/D to nearly 0. Therefore, these results are congruent with the ROC analysis without propensity score weighting. Due to the small sample size, the propensity score weighted AUC for Q-MRI was not calculated with cross-validation and might be slightly increased due to overfitting. However, comparing the unweighted AUC calculated with (0.76) or without (0.78) cross-validation, the effect of overfitting is expected to be small.

Impact of demographic, behavioral, and disease-related factors on MRI in CP participants

Table 3 shows the estimated regression coefficients and p-values of the covariates from the linear regression relating patient characteristics to each MRI parameter. This model was fitted to CP participants only because the calcification, EPD, and diabetes generally do not apply to the controls. Overall, these covariates showed little association with the MRI parameters.

Discussion

We evaluated the value of four quantitative MRI parameters for the diagnosis of CP in a prospective, multi-institutional setting using different hardware vendors. We hypothesized that; (a) loss of acinar cells and replacement by fibrosis would increase the T1 relaxation time due to a decline in the proteinaceous content, (b) measuring the ECV fraction would reflect replacement of acinar cells by fibrosis, and (c) a composite score of quantitative parameters would increase the diagnostic performance. Helpful parenchymal features were significantly higher in the CP group; T1 relaxation time, ECV fraction, and fat signal fraction. Each of these parameters showed moderately high diagnostic performance after adjustment for covariates. A Q-MRI score that combined these MR parameters improved diagnostic performance. ADC values derived from diffusion-weighted imaging were not helpful for the diagnosis of CP. We conclude that quantitative MRI parameters can serve as an imaging biomarker for evaluation of CP; however, further studies are needed using larger study populations, including acute and recurrent acute pancreatitis and longitudinal follow-ups.

The rationale for using the parenchymal features

The cardinal histopathologic features of CP are fibrosis, loss of acinar tissue, and ductal changes [1]. Cambridge classification used for MRCP primarily captures periductal fibrosis and does not directly assess the fibrosis in the rest of the parenchyma or loss of acinar cells. Since the pancreatic ductal system comprise only 4% of the normal pancreas [19, 20], the diagnosis of non-calcific CP can be elusive or delayed when using ductal imaging alone [21, 22]. MRI parenchymal signal changes may provide a more comprehensive evaluation of CP [6–8], potentially earlier detection of the pathophysiology, considering acinar cells comprise up to 85% of the normal pancreas [23]. Prior studies suggest that using ductal imaging has a moderate interobserver agreement [4] and using parenchymal imaging features may yield a more objective evaluation of CP [5]. Consensus guidelines highlighted the potential benefit of parenchymal imaging [6–8].

History of using T1 for evaluation of CP

The pancreas is a highly productive exocrine gland of the digestive system secreting more than 1–2 L of proteinaceous fluid per day containing digestive enzymes and bicarbonate [24, 25]. Attributed to the abundance of proteinaceous material in the acinar cells, the normal pancreas shows a relatively higher T1 signal intensity than other solid organs in the upper abdomen [26, 27]. Several publications reported the benefit of the T1 signal intensity ratio (SIR) for the diagnosis and staging of CP [22, 26–29]. Some studies reported correlation of the T1 SIR specifically with pancreatic exocrine dysfunction measured by the endoscopic pancreatic function tests [21, 28]. We identified three publications that correlated histopathology on surgical specimens with MRI parenchymal features (T1 SIR, T1 relaxation time, diffusion-weighted imaging, and MR elastography) [26, 30, 31]. These studies found a significant correlation of MRI parenchymal findings with the degree of fibrosis. Based on these reports, the T1 relaxation time reflects changes seen in histopathology.

The rationale for using quantitative MR imaging

The majority of the T1 and T2 sequences in clinical practice are not quantitative and are referred to as T1-weighted or T2-weighted images. There are limitations in conventional MR imaging in which the tissue contrast depends on multiple factors, including acquisition parameters, receiver coil geometry, and sensitivity and signal amplifier gains. Variation in signal intensity is commonly observed by choosing pulse sequence and manipulating acquisition parameters (e.g., flip angle, echo time, repetition time, inversion time, etc.). These limitations preclude direct comparison of intensity values among subjects or different time points. Quantitative MR techniques plot an image by measuring tissue-specific properties in each voxel [32]. This would allow a more useful interpretation of signal intensity changes with the benefit of cross-platform compatibility and a more accurate comparison when using longitudinal time points. These benefits give quantitative MRI the potential to be a non-invasive imaging biomarker for solid organ pathologies. A
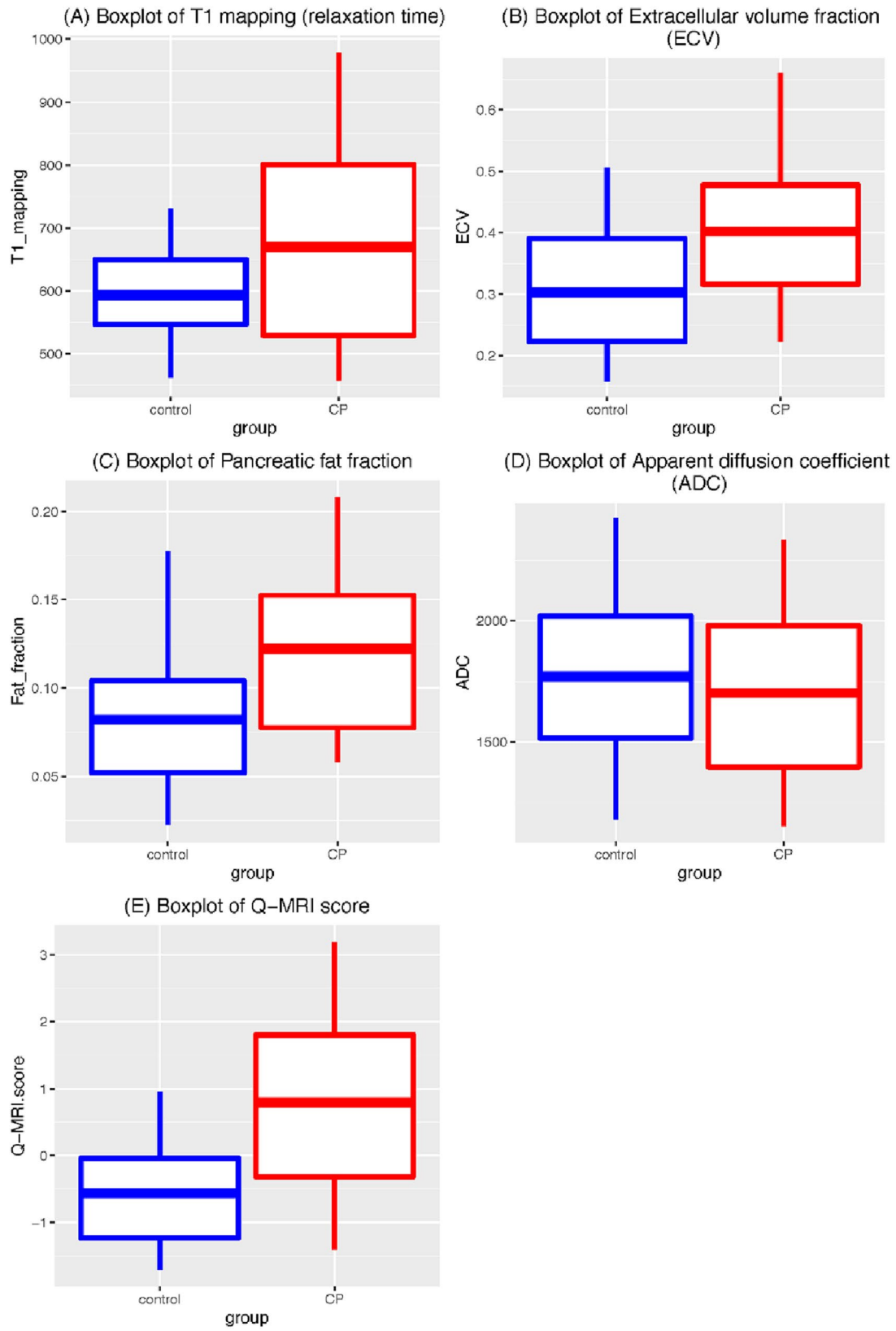
(A) Boxplot of T1 mapping (relaxation time)

(B) Boxplot of Extracellular volume fraction (ECV)

(C) Boxplot of Pancreatic fat fraction

(D) Boxplot of Apparent diffusion coefficient (ADC)

(E) Boxplot of Q–MRI score

◄**Fig. 3** Box-and-whisker plot of the four MRI parameters and Q-MRI score in control and CP groups. **a** T1 mapping (relaxation time in msec); **b** Extracellular volume (ECV) fraction; **c** Pancreatic fat signal fraction; **d** Apparent diffusion coefficient (ADC); **e** Q-MRI score of control and CP participants. T1 mapping ($p = 0.0056$), ECV ($p = 0.0004$), pancreatic fat signal fraction ($p = 0.0002$), and Q-MRI score ($p < 0.0001$) are statistically significantly different between controls and CP participants, but not ADC ($p = 0.4575$). The boxplots show the 25th and 75th quantiles and the mean

few quantitative MRI studies have been published reporting the alterations of T1 in a variety of pathologic conditions in the abdomen [10, 33, 34]. These studies focused on detecting tissue fibrosis, such as those seen with cirrhosis [35–37], CP [9], primary sclerosing cholangitis [38], and chronic kidney failure [39].

Extracellular volume fraction

The extracellular matrix increases due to adverse tissue remodeling leading to tissue fibrosis [10, 34]. It has been shown to be helpful for the evaluation of myocardial fibrosis [40–42] and cirrhosis [34, 37]. Since most of the current gadolinium-based contrast agents are extracellular during the late enhancement phase, T1 shortening of the tissues reflects their concentration in the extracellular space. Based on this pharmacokinetic property, ECV imaging can dichotomize tissues into their intracellular and extracellular components by using T1 relaxation times obtained before and after MR contrast enhancement. Further details of our ECV imaging methodology were previously published [12]. T1 and ECV values of the normal pancreas [43] and the usefulness of ECV imaging for the diagnosis of CP have been

previously reported [10]. The Higher ECV fraction seen in CP in this study agrees with previous publications.

Fatty infiltration and CP

Fatty infiltration (steatosis) can be seen in the liver, heart, and muscles due to metabolic changes (e.g., high triglycerides and free fatty acids) [44]. Histopathologic studies have reported evidence of fatty infiltration in CP [1, 45, 46]. Pancreatic steatosis has a reported prevalence of as high as two-thirds of individuals with type 2 diabetes [44]. Our results agree with previous publications that reported a higher fat signal fraction of the pancreas measured by MRI in CP patients [47].

Diffusion-weighted imaging

Apparent diffusion coefficient in this study were very similar in the control and CP groups. Our finding contrasts with prior study performed on 3.0 T [48] which reported higher values in healthy patients than in either mild or severe CP groups ($P < 0.01$). It is well known that diffusion-weighted imaging is highly dependent on the imaging parameters as well the magnet strength. Therefore, it is difficult to do a direct comparison of two studies performed using different imaging parameters and magnet strength.

Caveats

There are various T1 mapping sequences available for use [49]. We used 3D dual flip angle gradient echo technique, which is more suitable for abdominal imaging since

Table 2 MRI parameters and Q-MRI score in controls and participants with CP

	Controls ($n = 50$) Mean (SD, Q25, Q50, Q75)	Definite CP ($n = 51$) Mean (SD, Q25, Q50, Q75)	p-value*	AUC
T1 relaxation time (msec)	593 (81.9, 546.8, 593.1, 649.5)	669 (170.6, 529.3, 673.4, 800.7)	0.006	0.618
ECV fraction (%)	30.3 (11.9, 22.3, 27.9, 39.0)[1]	40.2 (14.7, 31.6, 37.9, 47.7)[1]	<0.001	0.715
ADC (10^{-6} mm²/s)	1771 (404, 1517, 1797, 2019)[12]	1703 (434, 1399, 1773, 1981)[4]	0.458	0.538
Fat signal fraction (%)	8.2 (4.4, 5.2, 7.5, 10.4)[2]	12.2 (5.5, 7.7, 10.9, 15.2)[3]	<0.001	0.727
Q-MRI score	− 0.56 (0.86, − 1.24, − 0.61, − 0.04)	0.80 (1.46, − 0.32, 0.62, 1.81)	<0.001	0.760**

Data reported as mean (standard deviation, 25th quantile, median, 75th quantile)

Superscripts indicate the missing values

*Two-sample t-test

**This cross-validated AUC of the Q-MRI score was calculated by 200 bootstrap cross-validation

(A) ROC curve of the MRI parameters and Q–MRI* score

(B) ROC curve of the MRI parameters and Q–MRI* score adjusted by propensity score
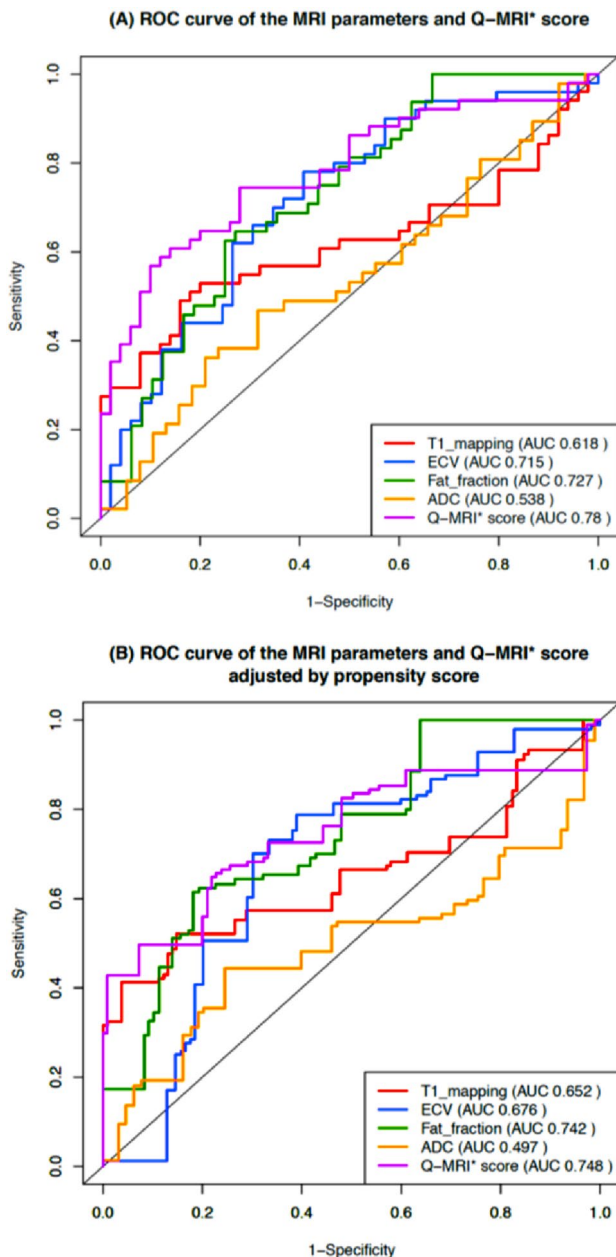

Fig. 4 ROC curve comparison of the four MRI parameters and the Q-MRI score with or without propensity score adjustment. ROC curve of T1 relaxation time, ECV fraction, ADC, pancreatic fat signal fraction, and Q-MRI score before **(a)** or after **(b)** propensity score adjustment. Q-MRI*: the ROC curve of Q-MRI is illustrated in this figure without cross-validation

it acquires volumetric T1 maps of the entire abdomen in one breath-hold [49]. If we used 2D T1 mapping techniques (e.g., MOLLI), we could only acquire three images of the abdomen per breath-hold [49]. While 3D imaging provides better spatial resolution, it may require B1 correction since it is sensitive to B1 + field inhomogeneity encountered over a large field of view, especially at higher magnetic field strengths [50]. Therefore, B1 correction was incorporated into our imaging protocol. Standardizing the quantitative imaging parameters was necessary by optimizing the dual flip angle selection across different scanners and manufacturers. We verified the correct flip angle selections by performing T1 phantom tests before certifying the accuracy of each scanner. ECV imaging is dependent on physiologic and imaging parameters (e.g., renal function, contrast dose, and delay time) [51] and also different relaxivity properties of gadolinium contrast agents [52] which can cause variability in measured T1 relaxation times. Our imaging protocol used the same contrast agent, manufacturer-recommended dosage, and 12-min delay time to avoid the influence of these factors [12].

The relatively smaller sample size was the main limitation of this pilot study. While we limited imaging to 1.5 T magnet strength, larger population studies in the future should allow evaluation using different magnet strengths.

Conclusion

Quantitative parenchymal imaging of the pancreas (T1 relation time, extracellular volume (ECV) fraction, and fat signal fraction) are helpful parameters that reflect the parenchymal changes in chronic pancreatitis (CP). Generating a quantitative MRI score by combining these parameters may increase diagnostic performance. Further studies are needed to validate these results in larger cohorts, including participants with acute and recurrent acute pancreatitis. The Consortium for the Study of Chronic Pancreatitis, Diabetes, and Pancreatic Cancer (CPDPC) is interested in assessing longitudinal trends in these MRI parameters to understand their utility as an imaging biomarker of disease progression. When tested in a high pre-test probability population, these imaging biomarkers are expected to be even more accurate. In future

Table 3 Linear regression models on the association between covariates and each of the four MRI parameters fitted to data from participants with established CP

	T1		ECV		Fat signal fraction		ADC	
	Estimate	*p*-value	Estimate	*p*-value	Estimate	*p*-value	Estimate	*p*-value
Intercept	955.5	<0.001	0.578	0.008*	0.036	0.640	2183.4	0.003*
Age (years)	− 2.63	0.153	− 0.001	0.524	0.001	0.231	− 0.466	0.934
Gender (Male vs. female)	− 130.8	0.025*	0.023	0.690	− 0.007	0.768	− 185.7	0.299
Race								
White vs. Asian	− 255.9	0.050	− 0.115	0.380	− 0.051	0.297	43.96	0.939
Black vs. Asian	− 23.0	0.895	− 0.238	0.188	− 0.050	0.454	− 321.4	0.621
BMI (kg/m^2)	3.16	0.560	− 0.002	0.706	0.003	0.236	− 11.74	0.520
Smoking								
Current vs Never	103.0	0.179	0.002	0.978	0.008	0.783	− 65.04	0.790
Past vs. Never	− 48.7	0.472	− 0.092	0.192	0.037	0.156	− 269.4	0.255
Drinking								
Current vs. Never	64.3	0.662	− 0.046	0.762	− 0.038	0.502	148.2	0.738
Past vs. Never	34.8	0.797	− 0.057	0.684	− 0.059	0.258	348.1	0.394
Drinking category								
Light vs Abstainer	− 37.6	0.782	0.073	0.607	0.065	0.223	− 112.9	0.781
Moderate vs Abstainer	− 65.5	0.627	0.099	0.476	0.068	0.200	− 35.10	0.934
Heavy vs. Abstainer	− 80.6	0.571	0.167	0.259	0.011	0.835	− 19.27	0.965
Very heavy vs. Abstainer	− 83.0	0.578	0.229	0.140	0.113	0.059	21.50	0.961
Diabetes (Yes, vs. No)	− 44.4	0.480	− 0.074	0.255	0.006	0.803	− 197.2	0.346
Calcification (Yes vs No)	190.9	0.004	0.028	0.668	− 0.025	0.312	19.94	0.920
EPD								
Yes vs. No	91.7	0.233	0.116	0.145	0.046	0.144	− 290.1	0.211
Not tested vs. No	− 63.7	0.312	0.030	0.638	0.051	0.040*	− 277.4	0.160

*Statistically significant at a critical value of 0.05

studies, combining these parenchymal features with ductal features should be explored to further increase the diagnostic performance.

Declarations

Conflict of interest All authors declare that they have no conflict of interest to disclose.

References

1. Esposito I, Hruban RH, Verbeke C, Terris B, Zamboni G, Scarpa A, et al. Guidelines on the histopathology of chronic pancreatitis. Recommendations from the working group for the international consensus guidelines for chronic pancreatitis in collaboration with the International Association of Pancreatology, the American Pancreatic Association, the Japan Pancreas Society, and the European Pancreatic Club. Pancreatology. 2020;20(4):586–93. doi: https://doi.org/10.1016/j.pan.2020.04.009.
2. Gardner TB, Adler DG, Forsmark CE, Sauer BG, Taylor JR, Whitcomb DC. ACG Clinical Guideline: Chronic Pancreatitis. Am J Gastroenterol. 2020;115(3):322-39. doi: https://doi.org/10.14309/ajg.0000000000000535.
3. Swensson J, Akisik F, Collins D, Olesen SS, Drewes AM, Frokjaer JB. Is Cambridge scoring in chronic pancreatitis the same using ERCP and MRCP?: A need for revision of standards. Abdom Radiol (NY). 2021;46(2):647-54. doi: https://doi.org/10.1007/s00261-020-02685-2.

4. Tirkes T, Shah ZK, Takahashi N, Grajo JR, Chang ST, Wachsman AM, et al. Inter-observer variability of radiologists for Cambridge classification of chronic pancreatitis using CT and MRCP: results from a large multi-center study. Abdom Radiol (NY). 2020;45(5):1481-7. doi: https://doi.org/10.1007/s00261-020-02521-7.

5. Trout AT, Abu-El-Haija M, Anupindi SA, Marine MB, Murati M, Phelps AS, et al. Interobserver Agreement for CT and MRI Findings of Chronic Pancreatitis in Children: A Multicenter Ancillary Study Under the INSPPIRE Consortium. American Journal of Roentgenology. 2022. doi: https://doi.org/10.2214/AJR.21.27234.

6. Steinkohl E, Olesen SS, Mark EB, Hansen TM, Frandsen LK, Drewes AM, et al. Progression of parenchymal and ductal findings in patients with chronic pancreatitis: A 4-year follow-up MRI study. Eur J Radiol. 2020;125:108868. doi: https://doi.org/10.1016/j.ejrad.2020.108868.

7. Tirkes T, Shah ZK, Takahashi N, Grajo JR, Chang ST, Venkatesh SK, et al. Reporting Standards for Chronic Pancreatitis by Using CT, MRI, and MR Cholangiopancreatography: The Consortium for the Study of Chronic Pancreatitis, Diabetes, and Pancreatic Cancer. Radiology. 2019;290(1):207-15. doi: https://doi.org/10.1148/radiol.2018181353.

8. Frokjaer JB, Akisik F, Farooq A, Akpinar B, Dasyam A, Drewes AM, et al. Guidelines for the Diagnostic Cross Sectional Imaging and Severity Scoring of Chronic Pancreatitis. Pancreatology. 2018;18(7):764-73. doi: https://doi.org/10.1016/j.pan.2018.08.012.

9. Tirkes T, Lin C, Fogel EL, Sherman SS, Wang Q, Sandrasegaran K. T1 mapping for diagnosis of mild chronic pancreatitis. J Magn Reson Imaging. 2017;45(4):1171-6. doi: https://doi.org/10.1002/jmri.25428.

10. Tirkes T, Lin C, Cui E, Deng Y, Territo PR, Sandrasegaran K, et al. Quantitative MR Evaluation of Chronic Pancreatitis: Extracellular Volume Fraction and MR Relaxometry. AJR Am J Roentgenol. 2018;210(3):533-42. doi: https://doi.org/10.2214/AJR.17.18606.

11. Rosenkrantz AB, Mendiratta-Lala M, Bartholmai BJ, Ganeshan D, Abramson RG, Burton KR, et al. Clinical utility of quantitative imaging. Acad Radiol. 2015;22(1):33-49. doi: https://doi.org/10.1016/j.acra.2014.08.011.

12. Tirkes T, Yadav D, Conwell DL, Territo PR, Zhao X, Venkatesh SK, et al. Magnetic resonance imaging as a non-invasive method for the assessment of pancreatic fibrosis (MINIMAP): a comprehensive study design from the consortium for the study of chronic pancreatitis, diabetes, and pancreatic cancer. Abdom Radiol (NY). 2019;44(8):2809-21. doi: https://doi.org/10.1007/s00261-019-02049-5.

13. The Consortium for the Study of Chronic Pancreatitis, Diabetes and Pancreatic Cancer (CPDPC) https://cpdpc.mdanderson.org (2015). Accessed.

14. Serrano J, Andersen DK, Forsmark CE, Pandol SJ, Feng Z, Srivastava S, et al. Consortium for the Study of Chronic Pancreatitis, Diabetes, and Pancreatic Cancer: From Concept to Reality. Pancreas. 2018;47(10):1208-12. doi: https://doi.org/10.1097/MPA.0000000000001167.

15. Yadav D, Park WG, Fogel EL, Li L, Chari ST, Feng Z, et al. PROspective Evaluation of Chronic Pancreatitis for EpidEmiologic and Translational StuDies: Rationale and Study Design for PROCEED From the Consortium for the Study of Chronic Pancreatitis, Diabetes, and Pancreatic Cancer. Pancreas. 2018;47(10):1229-38. doi: https://doi.org/10.1097/MPA.0000000000001170.

16. Pepe MS. The statistical evaluation of medical tests for classification and prediction. Oxford statistical science series, vol 28. Oxford ; New York: Oxford University Press; 2003.

17. Le Borgne F, Combescure C, Gillaizeau F, Giral M, Chapal M, Giraudeau B, et al. Standardized and weighted time-dependent receiver operating characteristic curves to evaluate the intrinsic prognostic capacities of a marker by taking into account confounding factors. Stat Methods Med Res. 2018;27(11):3397-410. doi: https://doi.org/10.1177/0962280217702416.

18. Imai K, Ratkovic M. Covariate Balancing Propensity Score. Journal of the Royal Statistical Society: Series B. 2014;76(1):243-63.

19. Barreto SG, Carati CJ, Toouli J, Saccone GT. The islet-acinar axis of the pancreas: more than just insulin. Am J Physiol Gastrointest Liver Physiol. 2010;299(1):G10-22. doi: https://doi.org/10.1152/ajpgi.00077.2010.

20. Tang X, Kusmartseva I, Kulkarni S, Posgai A, Speier S, Schatz DA, et al. Image-Based Machine Learning Algorithms for Disease Characterization in the Human Type 1 Diabetes Pancreas. Am J Pathol. 2021;191(3):454-62. doi: https://doi.org/10.1016/j.ajpath.2020.11.010.

21. Tirkes T, Fogel EL, Sherman S, Lin C, Swensson J, Akisik F, et al. Detection of exocrine dysfunction by MRI in patients with early chronic pancreatitis. Abdom Radiol (NY). 2017;42(2):544-51. doi: https://doi.org/10.1007/s00261-016-0917-2.

22. Balci NC, Alkaade S, Magas L, Momtahen AJ, Burton FR. Suspected chronic pancreatitis with normal MRCP: findings on MRI in correlation with secretin MRCP. J Magn Reson Imaging. 2008;27(1):125-31. doi: https://doi.org/10.1002/jmri.21241.

23. Atkinson MA, Campbell-Thompson M, Kusmartseva I, Kaestner KH. Organisation of the human pancreas in health and in diabetes. Diabetologia. 2020;63(10):1966-73. doi: https://doi.org/10.1007/s00125-020-05203-7.

24. Ishiguro H, Yamamoto A, Nakakuki M, Yi L, Ishiguro M, Yamaguchi M, et al. Physiology and pathophysiology of bicarbonate secretion by pancreatic duct epithelium. Nagoya J Med Sci. 2012;74(1-2):1-18.

25. Pandol SJ. Water and Ion Secretion from the Pancreatic Ductal System. The Exocrine Pancreas. Morgan & Claypool Life Sciences; 2010.

26. Watanabe H, Kanematsu M, Tanaka K, Osada S, Tomita H, Hara A, et al. Fibrosis and postoperative fistula of the pancreas: correlation with MR imaging findings--preliminary results. Radiology. 2014;270(3):791-9. doi: https://doi.org/10.1148/radiol.13131194.

27. Winston CB, Mitchell DG, Outwater EK, Ehrlich SM. Pancreatic signal intensity on T1-weighted fat saturation MR images: clinical correlation. J Magn Reson Imaging. 1995;5(3):267-71. doi: https://doi.org/10.1002/jmri.1880050307.

28. Balci NC, Smith A, Momtahen AJ, Alkaade S, Fattahi R, Tariq S, et al. MRI and S-MRCP findings in patients with suspected chronic pancreatitis: correlation with endoscopic pancreatic function testing (ePFT). J Magn Reson Imaging. 2010;31(3):601-6. doi: https://doi.org/10.1002/jmri.22085.

29. Gallix BP, Bret PM, Atri M, Lecesne R, Reinhold C. Comparison of qualitative and quantitative measurements on unenhanced T1-weighted fat saturation MR images in predicting pancreatic pathology. J Magn Reson Imaging. 2005;21(5):583-9. doi: https://doi.org/10.1002/jmri.20310.

30. Trikudanathan G, Walker SP, Munigala S, Spilseth B, Malli A, Han Y, et al. Diagnostic Performance of Contrast-Enhanced MRI With Secretin-Stimulated MRCP for Non-Calcific Chronic Pancreatitis: A Comparison With Histopathology. Am J Gastroenterol. 2015;110(11):1598-606. doi: https://doi.org/10.1038/ajg.2015.297.

31. Liu C, Shi Y, Lan G, Xu Y, Yang F. Evaluation of Pancreatic Fibrosis Grading by Multiparametric Quantitative Magnetic Resonance Imaging. J Magn Reson Imaging. 2021;54(5):1417-29. doi: https://doi.org/10.1002/jmri.27626.

32. Deoni SC. Quantitative relaxometry of the brain. Top Magn Reson Imaging. 2010;21(2):101-13. doi: https://doi.org/10.1097/RMR.0b013e31821e56d8.

33. Moon JC, Messroghli DR, Kellman P, Piechnik SK, Robson MD, Ugander M, et al. Myocardial T1 mapping and extracellular volume quantification: a Society for Cardiovascular Magnetic Resonance (SCMR) and CMR Working Group of the European Society of Cardiology consensus statement. J Cardiovasc Magn Reson. 2013;15:92. doi: https://doi.org/10.1186/1532-429X-15-92.

34. Ou HY, Bonekamp S, Bonekamp D, Corona-Villalobos CP, Torbenson MS, Geiger B, et al. MRI arterial enhancement fraction in hepatic fibrosis and cirrhosis. AJR Am J Roentgenol. 2013;201(4):W596-602. doi: https://doi.org/10.2214/AJR.12.10048.

35. Kim KA, Park MS, Kim IS, Kiefer B, Chung WS, Kim MJ, et al. Quantitative evaluation of liver cirrhosis using T1 relaxation time with 3 tesla MRI before and after oxygen inhalation. J Magn Reson Imaging. 2012;36(2):405-10. doi: https://doi.org/10.1002/jmri.23620.

36. Curtis WA, Fraum TJ, An H, Chen Y, Shetty AS, Fowler KJ. Quantitative MRI of Diffuse Liver Disease: Current Applications and Future Directions. Radiology. 2019;290(1):23-30. doi: https://doi.org/10.1148/radiol.2018172765.

37. Luetkens JA, Klein S, Traber F, Schmeel FC, Sprinkart AM, Kuetting DLR, et al. Quantification of Liver Fibrosis at T1 and T2 Mapping with Extracellular Volume Fraction MRI: Preclinical Results. Radiology. 2018;288(3):748-54. doi: https://doi.org/10.1148/radiol.2018180051.

38. Evrimler S, Swensson JK, Are VS, Tirkes T, Vuppalanchi R, Akisik F. Quantitative assessment of disease severity of primary sclerosing cholangitis with T1 mapping and extracellular volume imaging. Abdom Radiol (NY). 2021;46(6):2433-43. doi: https://doi.org/10.1007/s00261-020-02839-2.

39. Huang Y, Sadowski EA, Artz NS, Seo S, Djamali A, Grist TM, et al. Measurement and comparison of T1 relaxation times in native and transplanted kidney cortex and medulla. J Magn Reson Imaging. 2011;33(5):1241-7. doi: https://doi.org/10.1002/jmri.22543.

40. Kellman P, Wilson JR, Xue H, Bandettini WP, Shanbhag SM, Druey KM, et al. Extracellular volume fraction mapping in the myocardium, part 2: initial clinical experience. J Cardiovasc Magn Reson. 2012;14:64. doi: https://doi.org/10.1186/1532-429X-14-64.

41. Schelbert EB, Messroghli DR. State of the Art: Clinical Applications of Cardiac T1 Mapping. Radiology. 2016;278(3):658-76. doi: https://doi.org/10.1148/radiol.2016141802.

42. Ugander M, Oki AJ, Hsu LY, Kellman P, Greiser A, Aletras AH, et al. Extracellular volume imaging by magnetic resonance imaging provides insights into overt and sub-clinical myocardial pathology. Eur Heart J. 2012;33(10):1268-78. doi: https://doi.org/10.1093/eurheartj/ehr481.

43. Tirkes T, Mitchell JR, Li L, Zhao X, Lin C. Normal T1 relaxometry and extracellular volume of the pancreas in subjects with no pancreas disease: correlation with age and gender. Abdom Radiol (NY). 2019;44(9):3133-8. doi: https://doi.org/10.1007/s00261-019-02071-7.

44. Lee JS, Kim SH, Jun DW, Han JH, Jang EC, Park JY, et al. Clinical implications of fatty pancreas: correlations between fatty pancreas and metabolic syndrome. World J Gastroenterol. 2009;15(15):1869-75. doi: https://doi.org/10.3748/wjg.15.1869.

45. Kloppel G. Chronic pancreatitis, pseudotumors and other tumor-like lesions. Mod Pathol. 2007;20 Suppl 1:S113-31. doi: https://doi.org/10.1038/modpathol.3800690.

46. Singhi AD, Pai RK, Kant JA, Bartholow TL, Zeh HJ, Lee KK, et al. The histopathology of PRSS1 hereditary pancreatitis. Am J Surg Pathol. 2014;38(3):346-53. doi: https://doi.org/10.1097/PAS.0000000000000164.

47. Tirkes T, Jeon CY, Li L, Joon AY, Seltman TA, Sankar M, et al. Association of Pancreatic Steatosis With Chronic Pancreatitis, Obesity, and Type 2 Diabetes Mellitus. Pancreas. 2019;48(3):420-6. doi: https://doi.org/10.1097/MPA.0000000000001252.

48. Akisik MF, Sandrasegaran K, Jennings SG, Aisen AM, Lin C, Sherman S, et al. Diagnosis of chronic pancreatitis by using apparent diffusion coefficient measurements at 3.0-T MR following secretin stimulation. Radiology. 2009;252(2):418–25. doi: https://doi.org/10.1148/radiol.2522081656.

49. Tirkes T, Zhao X, Lin C, Stuckey AJ, Li L, Giri S, et al. Evaluation of variable flip angle, MOLLI, SASHA, and IR-SNAPSHOT pulse sequences for T1 relaxometry and extracellular volume imaging of the pancreas and liver. MAGMA. 2019;32(5):559-66. doi: https://doi.org/10.1007/s10334-019-00762-2.

50. Cheng HL, Wright GA. Rapid high-resolution T(1) mapping by variable flip angles: accurate and precise measurements in the presence of radiofrequency field inhomogeneity. Magn Reson Med. 2006;55(3):566-74. doi: https://doi.org/10.1002/mrm.20791.

51. Gai N, Turkbey EB, Nazarian S, van der Geest RJ, Liu CY, Lima JA, et al. T1 mapping of the gadolinium-enhanced myocardium: adjustment for factors affecting interpatient comparison. Magn Reson Med. 2011;65(5):1407-15. doi: https://doi.org/10.1002/mrm.22716.

52. Huppertz A, Rohrer M. Gadobutrol, a highly concentrated MR-imaging contrast agent: its physicochemical characteristics and the basis for its use in contrast-enhanced MR angiography and perfusion imaging. Eur Radiol. 2004;14 Suppl 5:M12-8. doi: https://doi.org/10.1007/s10406-004-0048-7.

Authors and Affiliations

Temel Tirkes[1] · Dhiraj Yadav[2] · Darwin L. Conwell[3] · Paul R. Territo[4] · Xuandong Zhao[5] · Scott A. Persohn[6] · Anil K. Dasyam[7] · Zarine K. Shah[8] · Sudhakar K. Venkatesh[9] · Naoki Takahashi[9] · Ashley Wachsman[10] · Liang Li[11] · Yan Li[12] · Stephen J. Pandol[13] · Walter G. Park[14] · Santhi S. Vege[15] · Phil A. Hart[16] · Mark Topazian[17] · Dana K. Andersen[18] · Evan L. Fogel[19] · On behalf of the Consortium for the Study of Chronic Pancreatitis, Diabetes, Pancreatic Cancer (CPDPC)

✉ Temel Tirkes
   atirkes@iu.edu

   Dhiraj Yadav
   yadavd@upmc.edu

   Darwin L. Conwell
   darwin.conwell@uky.edu

   Paul R. Territo
   pterrito@iupui.edu

   Xuandong Zhao
   zhaoxua@iu.edu

   Scott A. Persohn
   spersohn@iupui.edu

   Anil K. Dasyam
   dasyamak@upmc.edu

   Zarine K. Shah
   zarine.shah@osumc.edu

   Sudhakar K. Venkatesh
   venkatesh.sudhakar@mayo.edu

   Naoki Takahashi
   Takahashi.Naoki@mayo.edu

   Ashley Wachsman
   Ashley.Wachsman@cshs.org

   Liang Li
   lli15@mdanderson.org

   Yan Li
   Yan.Li.1@uth.tmc.edu

   Stephen J. Pandol
   stephen.pandol@cshs.org

   Walter G. Park
   wgpark@stanford.edu

   Santhi S. Vege
   vege.santhi@mayo.edu

   Phil A. Hart
   philip.hart@osumc.edu

   Mark Topazian
   topazian@gmail.com

   Dana K. Andersen
   dana.andersen@nih.gov

   Evan L. Fogel
   efogel@iu.edu

[1]   Department of Radiology and Imaging Sciences, Indiana University School of Medicine Indianapolis, 550 N. University Blvd. Suite 0663, Indianapolis, IN 46202, USA

[2]   Department of Medicine Division of Gastroenterology, Hepatology & Nutrition University of Pittsburgh School of Medicine, Pittsburgh, PA, USA

[3]   Department of Internal Medicine, University of Kentucky College of Medicine, Lexington, KY, USA

[4]   Division of Clinical Pharmacology, Stark Neurosciences Research Institute Radiology and Imaging Sciences, Indiana University School of Medicine, Indianapolis, IN 46202, USA

[5]   Department of Radiology and Imaging Sciences, Indiana University School of Medicine, Indianapolis, IN 46202, USA

[6]   Stark Neurosciences Research Institute, Indiana University School of Medicine, Indianapolis, IN 46202, USA

[7]   Department of Radiology, University of Pittsburgh Medical Center, Pittsburgh, PA, USA

[8]   Department of Radiology, The Ohio State University Wexner Medical Center, Columbus, OH, USA

[9]   Department of Radiology, Mayo Clinic, Rochester, MN, USA

[10] Department of Radiology Cedars-Sinai Medical Center, University of California in Los Angeles, Los Angeles, CA, USA

[11] Department of Biostatistics Director, Quantitative Science Program, The University of Texas MD Anderson Cancer Center, Houston, TX, USA

[12] Department of Biostatistics, The University of Texas MD Anderson Cancer Center, Houston, TX, USA

[13] Division of Digestive and Liver Diseases Cedars-Sinai Medical Center, Los Angeles, CA, USA

[14] Department of Medicine, Division of Gastroenterology and Hepatology, Stanford University Medical Center, Stanford, CA, USA

[15] Department of Internal Medicine, Mayo Clinic, Rochester, MN, USA

[16] Division of Gastroenterology, Hepatology & Nutrition The Ohio State University Wexner Medical Center, Columbus, OH, USA

[17] Mayo Clinic, Rochester, MN, USA

[18] Division of Digestive Diseases and Nutrition National Institute of Diabetes and Digestive and Kidney Diseases, National Institutes of Health, Bethesda, MD, USA

[19] Lehman, Bucksot and Sherman Section of Pancreatobiliary Endoscopy, Indiana University School of Medicine, Indianapolis, IN, USA